

Proceeding Paper

Fabrication and Characterization of Perovskite Solar Cells Using Copper Phthalocyanine Complex with Tetracyanoquinodimethane [†]

Atsushi Suzuki ^{1,*}, Ryota Hasegawa ¹, Takeo Oku ¹, Masanobu Okita ², Sakiko Fukunishi ², Tomoharu Tachikawa ² and Tomoya Hasegawa ²

¹ Department of Materials Science, The University of Shiga Prefecture, 2500 Hassaka, Hikone 522-8533, Japan; oe21rhasegawa@ec.usp.ac.jp (R.H.); oku@mat.usp.ac.jp (T.O.)

² Osaka Gas Chemicals Co., Ltd., 5-11-61 Torishima, Konohana-ku, Osaka 554-0051, Japan; okita@ogc.co.jp (M.O.); fukunishi@ogc.co.jp (S.F.); t-tachikawa@ogc.co.jp (T.T.); hasegawa_tomoya@ogc.co.jp (T.H.)

* Correspondence: suzuki@mat.usp.ac.jp; Tel.: +81-749-28-8369

[†] Presented at the 3rd International Online Conference on Crystals, 15–30 January 2022; Available online: https://iocc_2022.sciforum.net/.

Abstract: In this paper, the fabrication and characterization of CH₃NH₃PbI₃ perovskite solar cells using decaphenylpentacyclosilane, copper phthalocyanine complex (CuPc) doped with tetracyanoquinodimethane (TCNQ), was performed. The effects of a carboxylic acid, amino, or sulfonic acid sodium salt group, substituted with CuPc doped with TCNQ, on photovoltaic properties was investigated to improve carrier generation and diffusion related to short-circuit current density. The incorporation of carboxylic acid or amino, substituted with CuPc doped with TCNQ, would optimize the tuning energy levels of the valence band, promoting charge transfer and diffusion with a suppressing trap near the interface in the hole-transporting layer.

Keywords: perovskite solar cell; phthalocyanine; tetracyanoquinodimethane; photovoltaic properties; morphology



Citation: Suzuki, A.; Hasegawa, R.; Oku, T.; Okita, M.; Fukunishi, S.; Tachikawa, T.; Hasegawa, T.

Fabrication and Characterization of Perovskite Solar Cells Using Copper Phthalocyanine Complex with Tetracyanoquinodimethane. *Chem. Proc.* **2022**, *9*, 8. https://doi.org/10.3390/IOCC_2022-12154

Academic Editor: Arcady Zhukov

Published: 13 January 2022

Publisher's Note: MDPI stays neutral with regard to jurisdictional claims in published maps and institutional affiliations.



Copyright: © 2022 by the authors. Licensee MDPI, Basel, Switzerland. This article is an open access article distributed under the terms and conditions of the Creative Commons Attribution (CC BY) license (<https://creativecommons.org/licenses/by/4.0/>).

1. Introduction

Perovskite solar cells have high potential for practical use as next-generation solar cells with characteristics such as high-power conversion efficiency related to photovoltaic performance, and an easy manufacturing process [1–4]. Perovskite solar cells are constructed with a photo-active layer on the hole-transporting layers [5]. The photovoltaic properties are based on the perovskite crystal and chemical elements such as an organic cation; methyl ammonium (MA) [6], ethyl ammonium (EA) [7,8], formamidinium (FA) [9,10], guanidinium (GA) [11–13], phenyl ethyl ammonium (PEA) [14], *p*-phenylenediaminium [15], alkali metals (sodium, potassium, rubidium and cesium) [16] at the A-site; lead [17], tin, transition metals [18,19], lanthanide or rare earth ions [20,21] at the B-site; and a halogen anion at the X-site in the perovskite crystal. The photovoltaic characteristics of perovskite crystals with a tuning composition mole-ratio of chemical elements have been determined for improving conversion efficiency, morphologies, and crystal orientation. Photovoltaic performance is based on carrier diffusion, with the suppression of recombination and trapping near the defect, and interfaces between the crystal grains in the perovskite layer. The stability of photovoltaic performance is performed to suppress desorption of the organic cation and halogen anion. Control of composition ratio such as the organic cation, transition and alkali metals, and halogen atoms, and the development of alternative hole-transporting materials [22–25] have been performed for the application of photovoltaic devices.

Alternative hole-transporting materials using silane derivatives such as decaphenylcyclopentasilane (DPPS), in terms of a conventional hole-transporting material such as 2,2',7,7'-tetrakis(*N,N*-di-*p*-methoxyphenylamine)-9,9'-spirobifluorene (spiro-OMeTAD), have been developed for improving the stability of conversion efficiency while suppressing decomposition [26–29]. In addition, metal phthalocyanines, as organic semi-conductive materials, have an advantage in electronic devices such as organic solar cells and perovskite solar cells [30–42]. The photovoltaic properties of the metal phthalocyanine complex are based on electron structure and molecular modification. The addition of metal phthalocyanines into the perovskite layer promotes photo-induced carrier generation and charge diffusion related to mobility, with optimization of the surface morphology on the perovskite layer. Optimization by tuning the microstructure and morphologies in the perovskite layer is an important factor for improving the stability of the conversion efficiency. Metal phthalocyanine complex derivatives (MPc, M = Cu²⁺, Zn²⁺) doped with 7,7,8,8-tetracyanoquinodimethane (TCNQ) [43] have been used as an efficient hole-transporting material for improving carrier mobility related to short-circuit current density and conversion efficiency.

The purpose of this study is to fabricate and characterize perovskite solar cells using DPPS, with the addition of copper phthalocyanine complex derivatives (CuPcX₄) doped with TCNQ, as hole-transporting materials. In particular, the influence of a carboxylic acid, amino, or sulfonic acid sodium salt group substituted with CuPc doped with TCNQ on the photovoltaic properties was investigated. The photovoltaic properties were measured by current–voltage (*J*-*V*) curves under light irradiation. The photovoltaic properties are discussed using the experimental results.

2. Materials and Methods

The CH₃NH₃PbI₃ (MAPbI₃) perovskite solar cell, using DPPS and MPc doped with TCNQ, was fabricated using the following process: For the preparation of the solar cell substrate, F-doped tin oxide (FTO) substrates were cleaned using an ultrasonic bath with acetone and methanol, and dried under nitrogen gas. The 0.15 and 0.30 M TiO_x precursor solution was prepared from titanium diisopropoxide bis(acetylacetonate) (0.055 and 0.11 mL, Sigma-Aldrich, Tokyo, Japan) with 1-butanol (1 mL, Nacalai Tesque, Kyoto, Japan). The 0.15 M TiO_x precursor solution was spin-coated on the FTO substrate at 3000 rpm for 30 s and annealed at 125 °C for 5 min. Then, the 0.30 M TiO_x precursor solution was spin-coated on the TiO_x layer at 3000 rpm for 30 s and annealed at 125 °C for 5 min. This process using the 0.30 M solution was performed two times, and the FTO substrate was sintered at 500 °C for 30 min to form the compact TiO₂ layer. After that, TiO₂ paste was coated on the substrate by spin-coating at 5000 rpm for 30 s. For the formation of the mesoporous TiO₂ layer, the TiO₂ paste was prepared using TiO₂ powder (P-25, Aerosil, Tokyo, Japan) with polyethylene glycol (PEG #20000, Naalai Tesque, Kyoto, Japan) in ultrapure water. The solution was mixed with acetylacetone (10 μL, Fujifilm Wako Pure Chemical Corporation, Osaka, Japan) and triton X-100 (5 μL, Sigama-Aldrich, Tokyo, Japan) for 30 min, and was left for 12 h to suppress the bubbles in the solution. The cells were annealed at 120 °C for 5 min and at 500 °C for 30 min to form the mesoporous TiO₂ layer.

For the preparation of the perovskite compounds, a solution of CH₃NH₃I (MAI, 2.4 M, Tokyo Chemical Industry, Tokyo, Japan), and PbI₂ (0.8 M, Sigma-Aldrich, Tokyo, Japan) with a desired mole ratio in *N,N*-dimethylformamide (0.5 mL, Sigma-Aldrich, Tokyo, Japan) was mixed at 60 °C. The solution of perovskite compound was then introduced into the TiO₂ mesoporous using a spin-coating method. In the last stage of the spin coating, DPPS (OGSOL SI-30-15, Osaka Gas Chemicals, Osaka, Japan) as a hole-transport layer (HTL) was prepared using chlorobenzene (0.5 mL, Fujifilm Wako Pure Chemical Corporation, Osaka, Japan). The DPPS solutions were dropped on the perovskite layer during the last 15 s of spin-coating of the perovskite precursor solutions. The perovskite cells coated with the DPPS layer were annealed at 190 °C for 10 min.

As shown in Figure 1, copper (II) phthalocyanine complexes were used for preparation of the hole-transporting layer. A solution of copper (II) phthalocyanine tetracarboxylic

acid ($\text{CuPc}(\text{COOH})_4$, Orient Chemical Industries Co., Ltd. Osaka, Japan), copper (II) tetra(amino)phthalocyanine ($\text{CuPc}(\text{NH}_2)_4$, Orient Chemical Industries Co., Ltd. Osaka, Japan), and copper (II) phthalocyanine-tetra sulfonic acid tetrasodium salt ($\text{CuPc}(\text{SO}_3\text{Na})_4$, 18 mg, Sigma-Aldrich, Japan) mixed with TCNQ (2 mg, Sigma-Aldrich, Japan) in ethanol (1.0 mL, Nacalai Tesque, Kyoto, Japan) was prepared using spin-coating annealing at 110 °C for 10 min. As preparation of the standard hole-transporting layer took place, a solution of 2,2',7,7'-tetrakis[*N,N*-di(methoxyphenyl)amino]-9,9'-spirobifluorene (spiro-OMeTAD, 36.1 mg, Sigma-Aldrich, Tokyo, Japan) in chlorobenzene (0.5 mL, Fujifilm Wako Pure Chemical Corporation, Osaka, Japan) was mixed with a solution of lithium bis(trifluoromethylsulfonyl)imide (Li-TFSI, 260 mg, Tokyo Chemical Industry, Tokyo, Japan) in acetonitrile (0.5 mL, Sigma-Aldrich, Tokyo, Japan) for 24 h. The former solution, with 4-*tert*-butylpyridine (14.4 μL , Sigma-Aldrich, Tokyo, Japan), was mixed with the Li-TFSI solution (8.8 μL) for 30 min at 70 °C. All procedures were carried out in ordinary air. Finally, gold (Au) metal contacts were evaporated as top electrodes. The photovoltaic cells were fabricated with the layered structures of FTO/TiO₂/perovskite/DPPS/ CuPc-doped TCNQ/Au.

The *J-V* characteristics (Keysight B2901A, Keysight Technologies, Santa Rosa, CA, USA) of the photovoltaic cells were measured under illumination at 100 mW cm⁻² by using an AM 1.5 solar simulator (San-ei Electric XES-301S, Osaka, Japan). One substrate was fabricated and characterized for photovoltaic performance. The best and average conversion efficiencies, and standard deviations of the solar cells with the three electrodes prepared in this study, were measured in the reverse scan of the *J-V* curves. The solar cells were illuminated through the side of the FTO substrates, and the illuminated area was 0.090 cm².

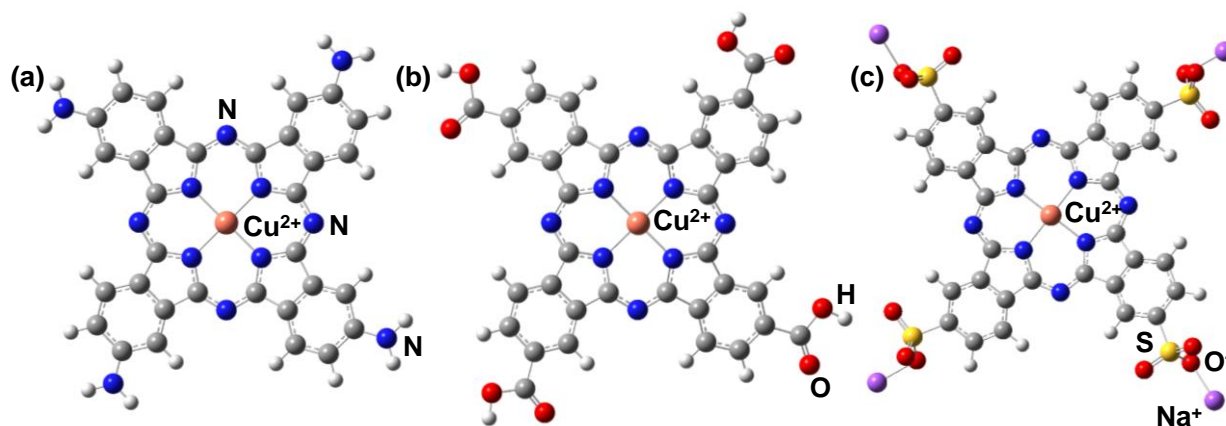


Figure 1. Molecular structures of copper (II) phthalocyanine complexes: (a) $\text{CuPc}(\text{NH}_2)_4$; (b) $\text{CuPc}(\text{COOH})_4$; and (c) $\text{CuPc}(\text{SO}_3\text{Na})_4$.

3. Results and Discussion

The *J-V* characteristics of the photovoltaic cells were measured as listed in Table 1. In the case of $\text{CuPc}(\text{COOH})_4$ doped with TCNQ, the photovoltaic parameters such as short-circuit current density (J_{SC}), fill factor (*FF*), series resistance (R_s), shunt resistance (R_{sh}), and conversion efficiency (η) were 16.8 mA cm⁻², 0.655 V, 0.491, 3.14 Ω cm², 152 Ω cm², and 5.49%, as listed in Table 1. The photovoltaic performance was improved through the incorporation of $\text{CuPc}(\text{COOH})_4$ doped with TCNQ, as compared with the photovoltaic parameters in other cases. In the case of $\text{CuPc}(\text{NH}_2)_4$ doped with TCNQ, the photovoltaic performance of η decreased to 3.76%. In the case of $\text{CuPc}(\text{SO}_3\text{Na})_4$ doped with TCNQ, the photovoltaic parameters of J_{sc} and V_{oc} decreased to 2.66 mA cm⁻² and 0.603 V, decreasing η by 0.75%. The *J-V* characteristics of the photovoltaic cells were measured after 30 days. In all cases, after 30 days, the photovoltaic parameters of J_{sc} , V_{oc} , and *FF* related to η were influenced by the incorporation of CuPcX_4 doped with TCNQ. In particular, the incorporation of $\text{CuPc}(\text{NH}_2)_4$ doped with TCNQ improved the photovoltaic parameters of

V_{oc} , FF, R_s , and R_{sh} , increasing η in the range of 6.41–6.55% after 30 days. The incorporation of $\text{CuPc}(\text{NH}_2)_4$ doped with TCNQ had the advantage as the hole-transporting layer with a remaining stability of η , instead of a conventional hole-transporting material using spiro-OMeTAD.

Table 1. Photovoltaic parameters of the perovskite solar cells as prepared.

Devices	J_{sc} (mA cm^{-2})	V_{oc} (V)	FF	R_s ($\Omega \text{ cm}^2$)	R_{sh} ($\Omega \text{ cm}^2$)	η (%)	η_{ave} (%)
$\text{CuPc}(\text{NH}_2)_4$ -TCNQ	8.39	0.716	0.626	6.90	5000	3.76	1.30
$\text{CuPc}(\text{COOH})_4$ -TCNQ	16.8	0.655	0.491	3.14	152	5.49	4.45
$\text{CuPc}(\text{SO}_3\text{Na})_4$ -TCNQ	2.66	0.603	0.465	11.6	1160	0.75	0.54

The photovoltaic properties depend on the carrier diffusion while suppressing recombination near the interface between the crystal grains in the perovskite layer. When the incorporation of CuPcX_4 doped with TCNQ was performed, the carrier generation and charge transfer promoted the suppression of recombination near the interface in the hole-transporting layer. The holes in the valence band of the perovskite layer charge-transferred the valence bands of DPPS, CuPcX_4 and TCNQ in the hole-transporting layer on the gold electrode as the cathode. The valence bands of the hole-transporting layer were tuned through the incorporation of CuPcX_4 , with electronic donation and withdrawal substitution. The carboxyl acid or amino substituted with CuPc doped with TCNQ optimized the energy levels of the valence band state, promoting charge transfer and diffusion with suppression of the trap near the interface in the hole-transporting layer. The V_{oc} of the perovskite solar cells was associated with the energy gap between the valence band of the perovskite layer and the conduction band of TiO_2 layer as an electron-transporting layer. The incorporation of $\text{CuPc}(\text{NH}_2)_4$ doped with TCNQ improved carrier diffusion while suppressing decomposition in the perovskite layer, yielding an increase in J_{sc} related to η . Compared to the conventional fabrication using spiro-OMeTAD, the fabrication method with the incorporation of CuPcX_4 doped with TCNQ has a great advantage for application in photovoltaic devices with its long-term durability of performance.

4. Conclusions

The fabrication and characterization of perovskite solar cells using DPPS, with the addition of CuPcX_4 doped with TCNQ, were performed to improve the stability of conversion efficiency. The effects of a carboxylic acid, amino, or sulfonic acid sodium salt group, substituted with CuPc doped with TCNQ, on photovoltaic properties were investigated, to improve the parameters of J_{sc} and V_{oc} related to η . The incorporation of carboxylic acid or amino substituted with CuPc doped with TCNQ optimizes the tuning of the energy levels of the valence band state, promoting charge transfer and diffusion while suppressing the trap near the interface in the hole-transporting layer. In particular, the incorporation of $\text{CuPc}(\text{NH}_2)_4$ doped with TCNQ improved the stability of η while suppressing decomposition in the perovskite layer.

Author Contributions: Conceptualization, A.S. and T.O.; methodology, R.H.; software, A.S.; validation, A.S., R.H. and T.O.; formal analysis, R.H.; investigation, R.H., M.O., S.F., T.T. and T.H.; resources, R.H.; data curation, R.H.; writing—original draft preparation, A.S.; writing—review and editing, T.O.; visualization, R.H.; supervision, T.O.; project administration, T.O.; funding acquisition, A.S. and T.O. All authors have read and agreed to the published version of the manuscript.

Funding: This research was supported by JSPS KAKENHI, grant number 21K05261.

Institutional Review Board Statement: Not applicable.

Informed Consent Statement: Not applicable.

Data Availability Statement: All data generated and analyzed during this study are included in this published article.

Acknowledgments: We wish to thank Yasuhiro Yamazaki from Orient Chemical Industries Co., Ltd. for supplying the copper phthalocyanine complex for use as hole-transforming materials.

Conflicts of Interest: The authors declare no conflict of interest.

References

1. Yoo, J.J.; Seo, G.; Chua, M.R.; Park, T.G.; Lu, Y.; Rotermund, F.; Kim, Y.-K.; Moon, C.S.; Jeon, N.J.; Correa-Baena, J.-P.; et al. Efficient perovskite solar cells via improved carrier management. *Nature* **2021**, *590*, 587–593. [[CrossRef](#)] [[PubMed](#)]
2. Jeong, J.; Kim, M.; Seo, J.; Lu, H.; Ahlawat, P.; Mishra, A.; Yang, Y.; Hope, M.A.; Eickemeyer, F.T.; Kim, M.; et al. Pseudo-halide anion engineering for α -FAPbI₃ perovskite solar cells. *Nature* **2021**, *592*, 381–385. [[CrossRef](#)] [[PubMed](#)]
3. Dong, Q.; Zhu, C.; Chen, M.; Jiang, C.; Guo, J.; Feng, Y.; Dai, Z.; Yadavalli, S.K.; Hu, M.; Cao, X.; et al. Interpenetrating interfaces for efficient perovskite solar cells with high operational stability and mechanical robustness. *Nat. Commun.* **2021**, *12*, 973. [[CrossRef](#)] [[PubMed](#)]
4. Kim, D.; Jung, H.J.; Park, I.J.; Larson, B.W.; Dunfield, S.P.; Xiao, C.; Kim, J.; Tong, J.; Boonmongkolras, P.; Ji, S.G.; et al. Efficient, stable silicon tandem cells enabled by anion-engineered wide-bandgap perovskites. *Science* **2020**, *368*, 155–160. [[CrossRef](#)]
5. Gao, B.; Meng, J. RbCs(MAFA)PbI₃ perovskite solar cell with 22.81% efficiency using the precise ions cascade regulation. *Appl. Surf. Sci.* **2020**, *530*, 147240. [[CrossRef](#)]
6. Sun, P.-P.; Kripalani, D.R.; Chi, W.; Snyder, S.A.; Zhou, K. High carrier mobility and remarkable photovoltaic performance of two-dimensional Ruddlesden–Popper organic–inorganic metal halides (PA)₂(MA)₂M₃I₁₀ for perovskite solar cell applications. *Mater. Today* **2021**, *47*, 45–52. [[CrossRef](#)]
7. Liu, Z.; Qiu, L.; Ono, L.K.; He, S.; Hu, Z.; Jiang, M.; Tong, G.; Wu, Z.; Jiang, Y.; Son, D.-Y.; et al. A holistic approach to interface stabilization for efficient perovskite solar modules with over 2,000-hour operational stability. *Nat. Energy* **2020**, *5*, 596–604. [[CrossRef](#)]
8. Nishi, K.; Oku, T.; Kishimoto, T.; Ueoka, N.; Suzuki, A. Photovoltaic Characteristics of CH₃NH₃PbI₃ Perovskite Solar Cells Added with Ethylammonium Bromide and Formamidinium Iodide. *Coatings* **2020**, *10*, 410. [[CrossRef](#)]
9. Lyu, M.; Park, N.-G. Effect of Additives AX (A = FA, MA, Cs, Rb, NH₄, X = Cl, Br, I) in FAPbI₃ on Photovoltaic Parameters of Perovskite Solar Cells. *Sol. RRL* **2020**, *4*, 202000331. [[CrossRef](#)]
10. Kim, G.; Min, H.; Lee, K.S.; Lee, D.Y.; Yoon, S.M.; Seok, S.I. Impact of strain relaxation on performance of α -formamidinium lead iodide perovskite solar cells. *Science* **2020**, *370*, 108–112. [[CrossRef](#)]
11. Gao, L.; Li, X.; Liu, Y.; Fang, J.; Huang, S.; Spanopoulos, I.; Li, X.; Wang, Y.; Chen, L.; Yang, G.; et al. Incorporated Guanidinium Expands the CH₃NH₃PbI₃ Lattice and Enhances Photovoltaic Performance. *ACS Appl. Mater. Interfaces* **2020**, *12*, 43885–43891. [[CrossRef](#)] [[PubMed](#)]
12. Chavan, R.D.; Prochowicz, D.; Tavakoli, M.M.; Yadav, P.; Hong, C.K. Surface Treatment of Perovskite Layer with Guanidinium Iodide Leads to Enhanced Moisture Stability and Improved Efficiency of Perovskite Solar Cells. *Adv. Mater. Interfaces* **2020**, *7*, 2000105. [[CrossRef](#)]
13. Kishimoto, T.; Oku, T.; Suzuki, A.; Ueoka, N. Additive Effects of Guanidinium Iodide on CH₃NH₃PbI₃ Perovskite Solar Cells. *Phys. Status Solidi A* **2021**, *218*, 2100396. [[CrossRef](#)]
14. Liu, C.; Yang, Y.; Rakstys, K.; Mahata, A.; Franckevicius, M.; Mosconi, E.; Skackauskaite, R.; Ding, B.; Brooks, K.G.; Usiobo, O.J.; et al. Tuning structural isomers of phenylenediammonium to afford efficient and stable perovskite solar cells and modules. *Nat. Commun.* **2021**, *12*, 6394. [[CrossRef](#)] [[PubMed](#)]
15. Zardari, P.; Rostami, A.; Shekaari, H. p-Phenylenediaminium iodide capping agent enabled self-healing perovskite solar cell. *Sci. Rep.* **2020**, *10*, 20011. [[CrossRef](#)]
16. Chen, Y.; Li, N.; Wang, L.; Li, L.; Xu, Z.; Jiao, H.; Liu, P.; Zhu, C.; Zai, H.; Sun, M.; et al. Impacts of alkaline on the defects property and crystallization kinetics in perovskite solar cells. *Nat. Commun.* **2019**, *10*, 1112. [[CrossRef](#)]
17. Li, C.; Song, Z.; Chen, C.; Xiao, C.; Subedi, B.; Harvey, S.P.; Shrestha, N.; Subedi, K.K.; Chen, L.; Liu, D.; et al. Low-bandgap mixed tin–lead iodide perovskites with reduced methylammonium for simultaneous enhancement of solar cell efficiency and stability. *Nat. Energy* **2020**, *5*, 768–776. [[CrossRef](#)]
18. Ueoka, N.; Oku, T.; Suzuki, A. Additive effects of alkali metals on Cu-modified CH₃NH₃PbI_{3– δ} Cl _{δ} photovoltaic devices. *RSC Adv.* **2019**, *9*, 24231–24240. [[CrossRef](#)]
19. Suzuki, A.; Oku, T. Effects of transition metals incorporated into perovskite crystals on the electronic structures and magnetic properties by first-principles calculation. *Heliyon* **2018**, *4*, e00755. [[CrossRef](#)]
20. Song, Z.; Xu, W.; Wu, Y.; Liu, S.; Bi, W.; Chen, X.; Song, H. Incorporating of Lanthanides Ions into Perovskite Film for Efficient and Stable Perovskite Solar Cells. *Small* **2020**, *16*, 2001770. [[CrossRef](#)]
21. Suzuki, A.; Oku, T. Effects of mixed-valence states of Eu-doped FAPbI₃ perovskite crystals studied by first-principles calculation. *Mater. Adv.* **2021**, *2*, 2609–2616. [[CrossRef](#)]
22. Akman, E.; Shalan, A.E.; Sadegh, F.; Akin, S. Moisture-Resistant FAPbI₃ Perovskite Solar Cell with 22.25% Power Conversion Efficiency through Pentafluorobenzyl Phosphonic Acid Passivation. *ChemSusChem* **2020**, *14*, 1176–1183. [[CrossRef](#)] [[PubMed](#)]

23. Zhu, H.; Shen, Z.; Pan, L.; Han, J.; Eickemeyer, F.T.; Ren, Y.; Li, X.; Wang, S.; Liu, H.; Dong, X.; et al. Low-Cost Dopant Additive-Free Hole-Transporting Material for a Robust Perovskite Solar Cell with Efficiency Exceeding 21%. *ACS Energy Lett.* **2020**, *6*, 208–215. [[CrossRef](#)]
24. Wan, L.; Zhang, W.; Fu, S.; Chen, L.; Wang, Y.; Xue, Z.; Tao, Y.; Zhang, W.; Song, W.; Fang, J. Achieving over 21% efficiency in inverted perovskite solar cells by fluorinating a dopant-free hole transporting material. *J. Mater. Chem. A* **2020**, *8*, 6517–6523. [[CrossRef](#)]
25. Jeong, M.; Choi, I.W.; Go, E.M.; Cho, Y.; Kim, M.; Lee, B.; Jeong, S.; Jo, Y.; Choi, H.W.; Lee, J.; et al. Stable perovskite solar cells with efficiency exceeding 24.8% and 0.3-V voltage loss. *Science* **2020**, *369*, 1615–1620. [[CrossRef](#)] [[PubMed](#)]
26. Taguchi, M.; Suzuki, A.; Oku, T.; Ueoka, N.; Minami, S.; Okita, M. Effects of annealing temperature on decaphenylcyclopent silane-inserted $\text{CH}_3\text{NH}_3\text{PbI}_3$ perovskite solar cells. *Chem. Phys. Lett.* **2019**, *737*, 136822. [[CrossRef](#)]
27. Oku, T.; Kandori, S.; Taguchi, M.; Suzuki, A.; Okita, M.; Minami, S.; Fukunishi, S.; Tachikawa, T. Polysilane-Inserted Methylammonium Lead Iodide Perovskite Solar Cells Doped with Formamidinium and Potassium. *Energies* **2020**, *13*, 4776. [[CrossRef](#)]
28. Oku, T.; Taguchi, M.; Suzuki, A.; Kitagawa, K.; Asakawa, Y.; Yoshida, S.; Okita, M.; Minami, S.; Fukunishi, S.; Tachikawa, T. Effects of Polysilane Addition to Chlorobenzene and High Temperature Annealing on $\text{CH}_3\text{NH}_3\text{PbI}_3$ Perovskite Photovoltaic Devices. *Coatings* **2021**, *11*, 665. [[CrossRef](#)]
29. Suzuki, A.; Taguchi, M.; Oku, T.; Okita, M.; Minami, S.; Fukunishi, S.; Tachikawa, T. Additive effects of methyl ammonium bromide or formamidinium bromide in methylammonium lead iodide perovskite solar cells using decaphenylcyclopentasilane. *J. Mater. Sci. Mater. Electron.* **2021**, *32*, 26449–26464. [[CrossRef](#)]
30. Jiang, X.; Wang, D.; Yu, Z.; Ma, W.; Li, H.-B.; Yang, X.; Liu, F.; Hagfeldt, A.; Sun, L. Molecular Engineering of Copper Phthalocyanines: A Strategy in Developing Dopant-Free Hole-Transporting Materials for Efficient and Ambient-Stable Perovskite Solar Cells. *Adv. Energy Mater.* **2018**, *9*, 1803287. [[CrossRef](#)]
31. Matsuo, Y.; Ogumi, K.; Jeon, I.; Wang, H.; Nakagawa, T. Recent progress in porphyrin- and phthalocyanine-containing perovskite solar cells. *RSC Adv.* **2020**, *10*, 32678–32689. [[CrossRef](#)]
32. Yu, Z.; Wang, L.; Mu, X.; Chen, C.; Wu, Y.; Cao, J.; Tang, Y. Intramolecular Electric Field Construction in Metal Phthalocyanine as Dopant-Free Hole Transporting Material for Stable Perovskite Solar Cells with >21 % Efficiency. *Angew. Chem. Int. Ed.* **2021**, *60*, 6294–6299. [[CrossRef](#)] [[PubMed](#)]
33. Huang, P.; Hernández, A.; Kazim, S.; Ortiz, J.; Sastre-Santos, Á.; Ahmad, S. Molecularly engineered thienyl-triphenylamine substituted zinc phthalocyanine as dopant free hole transporting materials in perovskite solar cells. *Sustain. Energy Fuels* **2020**, *4*, 6188–6195. [[CrossRef](#)]
34. Molina, D.; Ruiz-Preciado, M.A.; Carlsen, B.; Eickemeyer, F.T.; Yang, B.; Flores-Díaz, N.; Álvaro-Martins, M.J.; Nonomura, K.; Hagfeldt, A.; Sastre-Santos, Á. Zinc Phthalocyanine Conjugated Dimers as Efficient Dopant-Free Hole Transporting Materials in Perovskite Solar Cells. *ChemPhotoChem* **2020**, *4*, 307–314. [[CrossRef](#)]
35. Javaid, S.; Lee, G. The impact of molecular orientation on carrier transfer characteristics at a phthalocyanine and halide perovskite interface. *RSC Adv.* **2021**, *11*, 31776–31782. [[CrossRef](#)] [[PubMed](#)]
36. Xiao, G.-B.; Wang, L.-Y.; Mu, X.-J.; Zou, X.-X.; Wu, Y.-Y.; Cao, J. Lead and Iodide Fixation by Thiol Copper(II) Porphyrin for Stable and Environmental-Friendly Perovskite Solar Cells. *CCS Chem.* **2021**, *3*, 25–36. [[CrossRef](#)]
37. Huang, P.; Hernández, A.; Kazim, S.; Follana-Berná, J.; Ortiz, J.; Lezama, L.; Sastre-Santos, Á.; Ahmad, S. Asymmetrically Substituted Phthalocyanines as Dopant-Free Hole Selective Layers for Reliability in Perovskite Solar Cells. *ACS Appl. Energy Mater.* **2021**, *4*, 10124–10135. [[CrossRef](#)]
38. Hu, Q.; Rezaee, E.; Xu, W.; Ramachandran, R.; Chen, Q.; Xu, H.; Assaad, T.E.; McGrath, D.V.; Xu, Z.X. Dual defect-passivation using phthalocyanine for enhanced efficiency and stability of perovskite solar cells. *Small* **2021**, *17*, 2005216. [[CrossRef](#)]
39. Esqueda, M.L.; Vergara, M.E.S.; Bada, J.R.; Salcedo, R. CuPc: Effects of its Doping and a Study of Its Organic-Semiconducting Properties for Application in Flexible Devices. *Materials* **2019**, *12*, 434. [[CrossRef](#)] [[PubMed](#)]
40. Suzuki, A.; Kida, T.; Takagi, T.; Oku, T. Effects of hole-transporting layers of perovskite-based solar cells. *Jpn. J. Appl. Phys.* **2016**, *55*, 2BF01. [[CrossRef](#)]
41. Suzuki, A.; Okumura, H.; Yamasaki, Y.; Oku, T. Fabrication and characterization of perovskite type solar cells using phthalocyanine complexes. *Appl. Surf. Sci.* **2019**, *488*, 586–592. [[CrossRef](#)]
42. Suzuki, A.; Hayashi, Y.; Yamasaki, Y.; Oku, T. Fabrication and characterization of perovskite solar cells added with zinc phthalocyanine to active layer. *AIP Conf. Proc.* **2019**, *2067*, 20010. [[CrossRef](#)]
43. Capitán, M.J.; Álvarez, J.; Navio, C. Study of the electronic structure of electron accepting cyano-films: TCNQversusTCNE. *Phys. Chem. Chem. Phys.* **2018**, *20*, 10450–10459. [[CrossRef](#)] [[PubMed](#)]